nzsee
NEW ZEALAND SOCIETY FOR EARTHQUAKE ENGINEERING

Experimental and analytical evaluation of different failure modes of self-centring braces

S.M.M. Yousef-beik & M. Seifi
Aurecon New Zealand Limited, Wellington.

P. Zarnani & S. Veismoradi

Auckland University of Technology, New Zealand, Auckland

A. Hashemi & P. Quenneville
University of Auckland, New Zealand, Auckland.

ABSTRACT

As resilience of structures during seismic events is currently a main structural engineering topic, Low-damage self-centring braces have the potential to serve this purpose by becoming a common low-damage lateral load resisting system. These systems have the capability to provide a considerable elastic stiffness, passive energy dissipation and self-centring characteristic. However, there is limited data available in the literature concerning their different failure modes and the associated design considerations. This paper summarizes the findings of the research program conducted at the Auckland University of Technology (AUT) and the University of Auckland (UoA) over the last four years on the performance of RSFJ low-damage self-centring brace. More specifically, the different failure modes, observed in the experimental programs, are classified, and a summary of the analytical formulations for their quantification and detection are provided. Finally, two flowcharts inclusive of the desirable hierarchical order of failure modes are proposed as a tool for the capacity design procedure by which, engineers can design the brace and the adjacent connections with respect to the intended level of shaking.

1 INTRODUCTION

RSFJ self-centring brace is relatively a new lateral load resisting system that was first introduced in 2018 [1-3]. This brace is mainly composed of three main elements: (i) Brace body, (ii) Damper and (iii) Telescopic tubes entitled Anti-buckling Tubes (ABTs) as depicted in Figure 1(a). As shown in the studies [1, 4, 5], this brace was susceptible to different types of elastic and inelastic buckling failure modes due to the rotational flexibility of the damper. Hashemi et al. [3] proposed an external jacket with a cross-section identical to that

of the brace body (see Figure 1 (b)) to be employed as the mechanism to postpone the buckling of the brace. However, this idea could not find its way into practice mainly because it had some practical implementation concerns regarding the installation of the jacket (for instance, in practice, normally the rods in the damper will become relatively long and will exceed the footprint of the brace and cannot be accommodated inside the jacket). Yousef-beik et al. [4], proposed a new mechanism to address those practical concerns using a male-female sliding telescopic configuration (entitled Anti-Buckling Tubes – ABTs – see Figure 1(c)). The major challenge for the implementation of this concept was the lack of a rational design procedure for the selection of the ABT sizes in a way that the global inelastic buckling capacity of the brace exceeds the intended demand. The challenge has been addressed by the proposed framework , and it was called SCMA (Simplified Collapse Mechanism Analysis) [6, 7].

In addition to the entire brace assembly studies, the damper performance under compression loads, was investigated further. It was found that the damper, itself, may experience either out-of-plane (Figure 1(d)) or in-plane (Figure 1(e)) buckling under special circumstances [8] like pinned-pinned installation. However, it was found that this can be simply remediated by changing one of the end connections to fixed or by employing stopper plates to limit the rotation of the damper and as a result hinder the buckling. Finally, the building seismic performance including the application of the proposed brace, in the performance enhancement of the conventional timber and steel structures was studied in [9-11]. The current paper provides a summary of the analytical and experimental investigations for the above-mentioned failure modes.

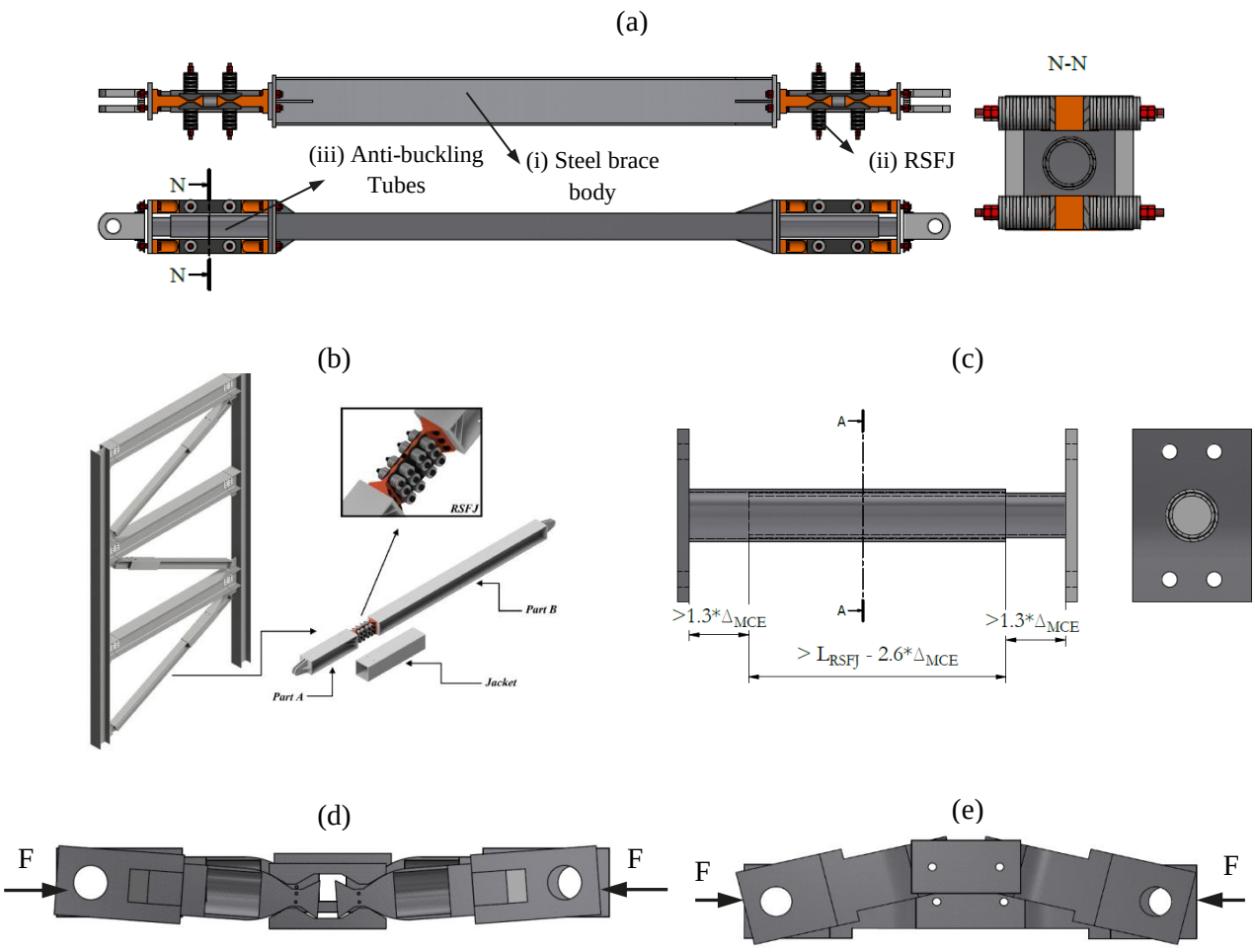

Figure 1: Self-centring RSFJ brace: (a) with internal sliding telescopic tubes (ABTs), (b) with external jacket, (c) ABTs details, (d & e) Localized out-of-plane and in-plane buckling of the damper

2 DIFFERENT FAILURE MODES IN COMPRESSION

In the subsequent text, the failure modes are categorized into two main groups in general namely: (a) local and (b) global instabilities. The local (localised) instability is associated with the damper being not able to transfer the axial compression fully while the global instability is referred to the whole brace sub-assembly being not able to resist the axial compression perfectly until the intended demand. In both cases, a premature failure is expected.

2.1 Global elastic and inelastic buckling

As for any member subjected to compression, the ultimate strength of the system in compression is highly dependent on the second-order ($P-\delta$) actions. In the common practice and code-compliant context, this is seen as an amplifier factor on the actions derived from the first-order elastic analysis.

In an ideal elastic system subjected to an incremental axial compression, the lateral displacement will increase due to the $P-\delta$ (shown by the curve with blue line in Figure 2(a)) where, the rate of this increase will even grow in the vicinity of the elastic buckling load. This is not the case when it comes to an elasto-plastic system in which the material has a limited strength. In fact, the weakest section in the system may fail during the increase of lateral deflection (black solid line in Figure 2). Depending on the geometry and the section properties, the strength can be less or equal to the elastic buckling load (slender or stocky members).

The ultimate strength can be simply approximated by intersecting two curves: the stiffness (blue dashed line) and strength (red dashed line) deterioration curves. If the intersection point is very close to the Euler load, the buckling will be referred to as *global elastic buckling* while if it is below the Euler load with considerable margin (like the case shown in Figure 2(a)), the buckling will be referred to as *global inelastic load*. It should be noted that in both cases of elastic and inelastic buckling, the ultimate strength would be reached, and the system would become a mechanism (statically unstable) when the required number of plastic hinges forms. The analytical closed-form framework for quantification of the ultimate compressive strength of the self-centring brace is discussed in detail [6, 7].

Figure 2(d) shows the different possible mechanism formations for a pinned-pinned brace that will be the case in either of the elastic or inelastic buckling cases. Because the system is pinned-pinned, only one plastic hinge is required so that the system develop a mechanism. Generally, there are two possible locations for the plastic hinge to form: (a) mid-span of the brace within the brace body (mechanism 1) and (b) end of the brace body within the ABT (mechanism 2).

Since the damper would be damaged due to the deformation compatibility with ABT present in mechanism 2, it is recommended that this mechanism be suppressed through the capacity design adoption. The analytical closed-form framework for detection of which mechanism is governing is presented below, yet for more info it can be referred to [6, 7].

As implied before, this method is based on the second-order plastic analysis, which is referred to as Simplified Collapse Mechanism Analysis (SCMA). In this method, whichever mechanisms that yields the lowest load (Figure 2(b)), will govern the design. In this regard, Equations 1-2 [7] provide the intersection points associated with the aforementioned mechanisms, and Equation 3 brings the ultimate strength of the brace in which M_p is the section capacity, P_{cr} is the elastic buckling load of the whole brace assembly, P_n is the axial section capacity and $\delta_0$is the initial imperfection of the system. The parameters and the procedure for their quantification are discussed in [7].

$$(\delta_{int})_{ABT} = 0.5(M_p)_{female}\left[\frac{1}{P_{cr}} + \sqrt{\left(\frac{1}{P_{cr}}\right)^2 + \frac{4\delta_0}{(M_p)_{female}.P_{cr}}}\right] \quad (1)$$

$$(\delta_{int})_{body} = 0.5(M_p)_{body}\left[\frac{1}{P_{cr}} - \frac{1}{P_n} + \sqrt{\left(\frac{1}{P_{cr}} - \frac{1}{P_n}\right)^2 + \frac{4\delta_0}{(M_p)_{body}.\ P_{cr}}}\right] \quad (2)$$

$$P_{ult} = \min\left[P_{cr} * \frac{(\delta_{int})_{ABT}}{(\delta_{int})_{ABT}+\delta_0},\ P_{cr} * \frac{(\delta_{int})_{body}}{(\delta_{int})_{body}+\delta_0}\right] \quad (3)$$

For the design purposes, it is recommended to select the section sizes (both brace body and ABTs) in a way that the *inelastic failure* mode is governed in a way to keep the ultimate strength close to the squash load P_n ($0.8P_n$-$0.95P_n$). By doing that, an optimal use of material can be achieved.

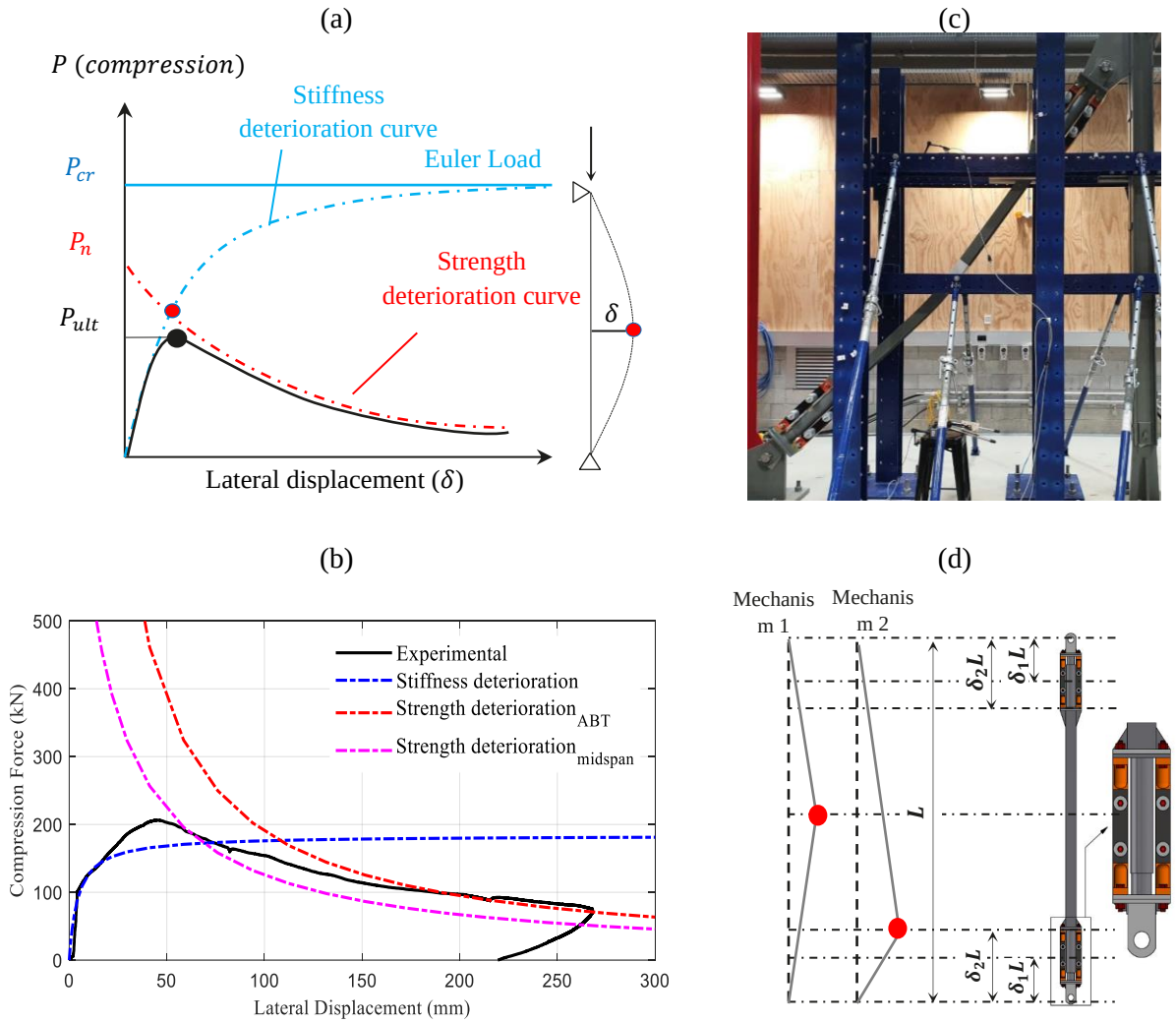

Figure 2: Experimental observation of global buckling: (a) theoretical behaviour [12], (b) experimental behaviour,(c) buckled shape of the brace and (d) different types of mechanism formation

2.2 Global nonlinear elastic buckling

The next failure mode is the global nonlinear elastic buckling. This failure mode will occur if no ABT is used within the brace and will occur in the in-plane direction of the damper (Figure 3) [1, 4, 5]. The reason for naming this failure mode as the *global nonlinear elastic* is that it firstly originates from the nonlinear elastic rotational behaviour of the damper in the in-plane direction [4] and secondly to make the reader alert on seeing the distinction between this failure mode and the one mentioned in the previous section. The failure load associated with this mode has been quantified and suggested as per Equations 4-6 [4, 5]:

$$P_{cr,loading} = \frac{n_b b^2 K_{stack}}{2\delta_1(1-\delta_1)L}\left(\frac{2sin^2\theta_g+\mu.sin2\theta_g}{2cos^2\theta_g-\mu.sin2\theta_g}\right) \quad (4)$$

$$P_{cr,unloading} = \frac{n_b b^2 K_{stack}}{2\delta_1(1-\delta_1)L}\left(\frac{2sin^2\theta_g-\mu.sin2\theta_g}{2cos^2\theta_g+\mu.sin2\theta_g}\right) \quad (5)$$

$$\Delta_{lat} \approx \sqrt{2\Delta_{axial}.L.\delta_1(1-\delta_1)} \quad (6)$$

in which $P_{cr,loading}$ and $P_{cr,unloading}$ are the approximate buckling loads in the loading and unloading phase, respectively. θ_g is the angle of grooves; μ is the coefficient of friction, n_b is the number of bolts on each splice, K_{stack} is stiffness of the stack of discs, b is the width of damper, $\delta_1$is the relative length of the damper shown in Figure 2(d), L is the total length of the brace and Δ_{lat} is the lateral displacement of the brace in case that it follows the zero-stiffness path (Figure 4). Regarding this failure mode, it should be mentioned that the behaviour is dependent on the quantity of the damper is pre-stressed force or in other words, slip force quantity of the damper.

According to a general stability rule [12, 13], when the axial load in a member approaches the buckling load ($P_{cr,loading}$), two equilibrium situations can exist for the member in the vicinity of the buckling load. The first situation is that the member buckles and the additional bending is resisted by the flexural strength of the member while in the second situation, the member does not buckle, and the additional axial load is resisted by the axial strength of the member. The first situation is referred to as *stable equilibrium* (no increase in axial force will be observed) while the second is referred to as *unstable equilibrium* (increase will be observed in axial load). This phenomenon is normally cited as the *bifurcation* in structural stability [13].

In case of the RSFJ-brace assembly and due to the presence of the pre-stressing force in the RSFJ, this bifurcation point can appear at the different levels of axial load. More specifically, depending on whether or not the slip force (F_{slip}) is higher than the buckling load ($P_{cr,loading}$), there can be two different behaviours associated with the brace.

In the *first case*, if the pre-stressing of the disc springs is relatively low in a way that the slip force is less than the critical load (shown in Figure 4(a) and Figure 4(b)), will be referred to as *low pre-stressed brace*, the bifurcation point (black filled circle) appears after-slip and is located at the intersection between $P_{cr,loading}$ and the flag-shape hysteresis curve (dark black line). At this specific point, the brace can follow two equilibrium paths. The first one (the continuous line) is the primary path (flag-shape), which is unstable (ball on a concave gravity field) after the buckling load and the RSFJ gets axially compacted in an unstable fashion. On the other hand, the second path is the dashed line during which the brace has a zero-lateral stiffness, so it exhibits a considerable lateral displacement, yet is stable (ball on a straight gravity field).

In the *second case*, shown in Figure 4(c) and Figure 4(d), if the pre-stressing of the disc springs is relatively high in a way that the slip force is higher than the critical load ($F_{slip} > P_{cr,loading}$), the bifurcation point is not located at the intersection between $P_{cr,loading}$ and the flag-shape curve (dark black line), and may appear exactly at the slip force or any higher force, which itself, depends on the imperfection of the system. The reason is that the prestressing force in the damper hinders the buckling and will postpone it to the after-slip situation. The difference to the previous case is that the system is always unstable after-slip because the axial force after slip is already beyond the buckling load. A more detailed discussion has been provided in [5] regarding the brace performance in the loading and unloading phase.

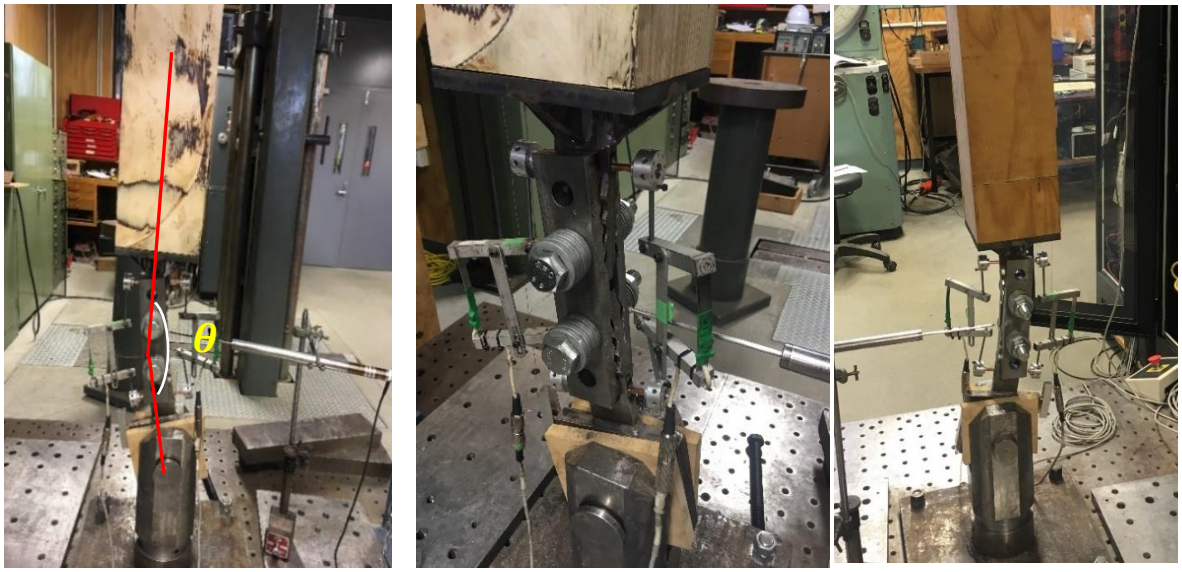

Figure 3: Experimental global nonlinear elastic buckling shape

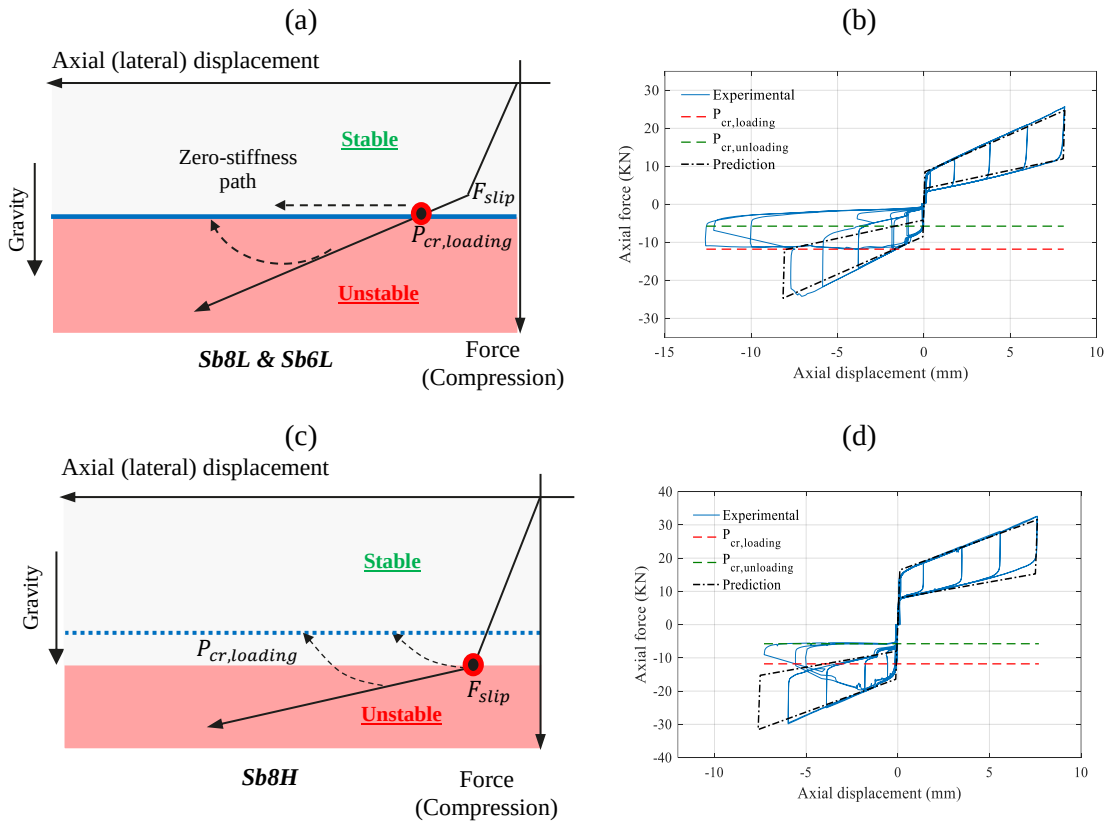

Figure 4: Different behaviour of brace: (a) When Slip force is less than critical load, (b) when Slip force is higher than the critical load

2.3 Localized buckling of the damper

The next failure mode is the local or localized damper buckling [8]. The reason for naming is that it tends to be similar to the local buckling of the steel sections in which a portion of the member would buckle independently of the adjacent parts and would interrupt the performance of the whole member. The main

consequence of this failure is the reduction of the axial capacity of the damper as shown in Figure 5(a) and Figure 5(c).

Regarding this failure mode, it was found that if the damper is installed with the pined-pined end conditions, a small amount of axial load eccentricity (or bending) is enough to trigger the failure and affect the axial capacity of the damper. However, it was observed that if one (or even both) of the boundary conditions is changed to fixed, this failure mode may not occur even with the load eccentricity.

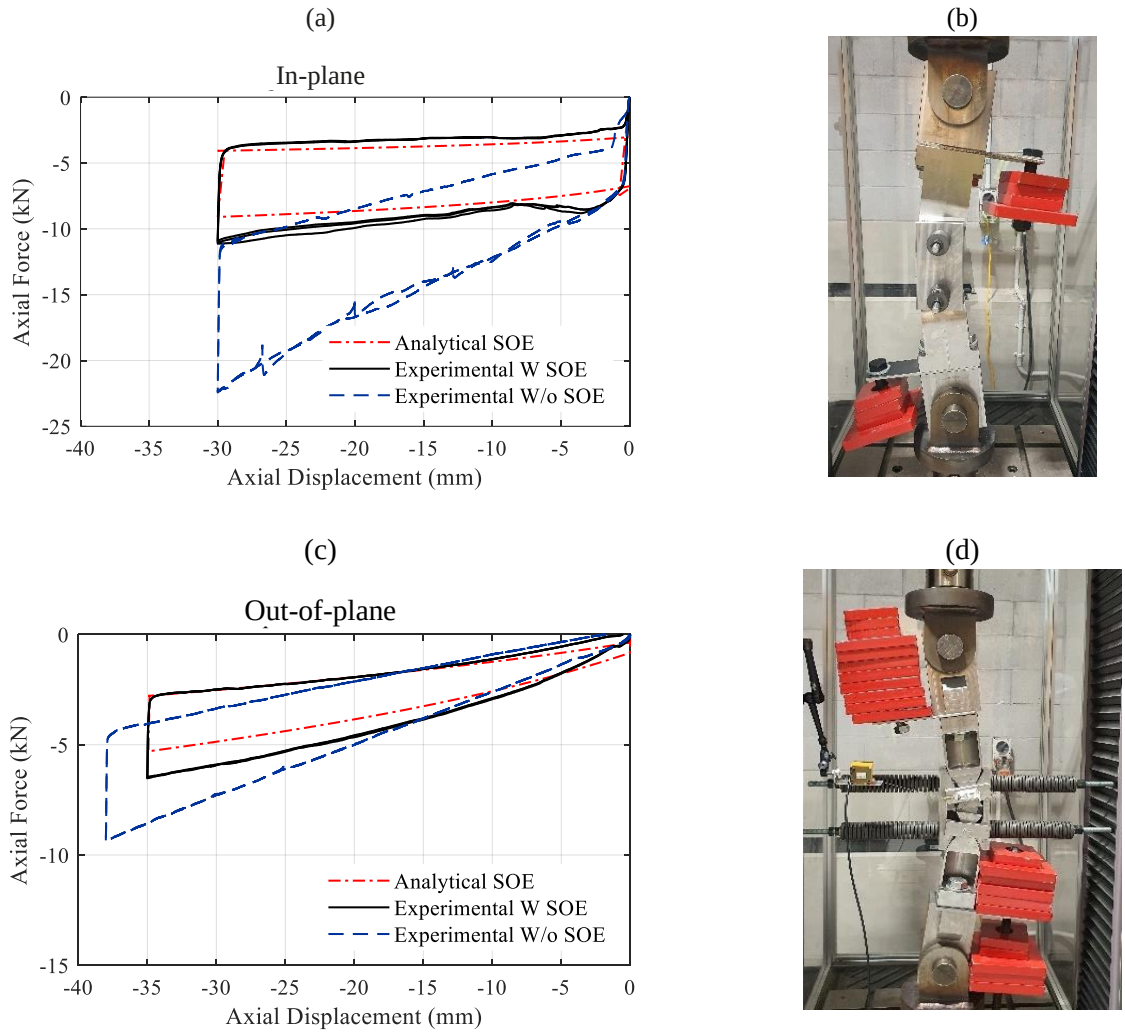

Figure 5: Local buckling of the damper with pinned-pinned boundary conditions: (a) in-plane observed experimental behaviour, (b) in-plane buckled mode shape, (c) Out-of-plane observed experimental behaviour and (d) out-of-plane buckled mode shape

3 ANTI-LOCKAGE MECHANISM (ALM)

There is a possibility that the displacement demand for the RSFJ exceeds the displacement capacity due to a major seismic event beyond the design level (ULS and MCE) and the disc spring becomes flat. If this happens, the damper may become locked, and the axial stiffness may increase rapidly (Figure 6(a)). This may induce a large inertial force into the structure and increase the force demand in members considerably.

A simple mechanism has been put forth entitled “Anti-locking mechanism (ALM) or secondary fuse” [3, 14, 15] in which the prestressing bolts (or rods) will start to yield when the disc springs become flat and the plastic deformation of the rods will provide more displacement capacity for the damper. Two simple equations regarding this failure mode are:

$$F_{flat,d} = F_{y,r} \quad (7)$$

$$\Delta_{additional}/\Delta_{ult,RSFJ} = \mu_{ALM} = \mu_r \tan(\theta_g) \quad (8)$$

Equation 7 shows that if the flattening force of the discs is equal to the yielding force of the rods, the damper will not lock at its ultimate condition, and Equation 8 shows that this extra deformation provided by the secondary fuse (anti-locking mechanism) is dependent on both the ductility of the rods (μ_r) and the angle of the grooves ($\tan(\theta_g)$) as shown in Figure 6(b). Regarding the self-centring capability of the damper, it should be mentioned that it will deteriorate but as long as the inelastic deformation of the rods is less than the displacement in the stack of discs due to the prestressing force, the static self-centring capability will be protected, otherwise, the disc would become loose, and a partial self-centring would occur. [15, 16].

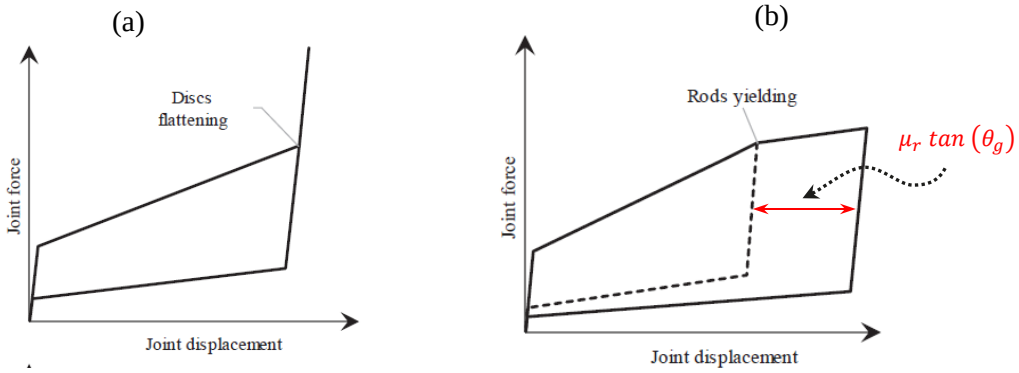

Figure 6: Damper performance at the ultimate limit state [15, 16]: (a) with lockage and (b) without lockage using secondary fuse (anti-locking mechanism)

4 DESIRABLE HIERARCHICAL ORDER OF FAILURES

For a better understanding of the readers and engineers when designing the brace, two flowcharts are proposed in Figure 7 which illustrates the hierarchical order of failure modes (or performance limit state) if they are sorted based on their desirability of occurrence with respect to an intended level of shaking (SLS, ULS and MCE). These flowcharts are expected to be used in conjunction with the capacity design procedure so that the sequence of each failure is respected. The first flowchart deals with the failure modes and the limit states when the brace is loaded in compression while the second one deals with the failure modes and the limit states when the brace is loaded in tension. As can be seen, both flowcharts are divided vertically into three subcategories namely: (i) ductile and damage-free phase, which includes the limit states/failure modes providing ductility and energy dissipation with no damage, (ii) ductile with damage, which includes the limit states/failure modes providing ductility but with structural damage and (iii) brittle failure modes. If the flowcharts are viewed horizontally, it can be noticed that a group of failures are associated with damper while other groups are concerned with the whole brace failure.

In terms of the level of shaking, as can be seen, it is recommended that the ULS level be assigned to the second vertical category (ductile with no damage). This insinuates that the activation of damper ALM can be set equal to the ULS level. Regarding the MCE, it is recommended that the MCE level is assigned to the first step of the third vertical category. This implies that the force demand at MCE level can be set equal to both overstrength force due to activation of ALM and the ultimate force due to buckling.

An extra important check is the safe margin between MCE and ULS. When checking Equation 8, it should be assured that the extra displacement provided by the ALM is 1.8-2 times larger than the damper ultimate point:

$$\mu_{ALM} \geq 1.8\text{-}2 \quad (9)$$

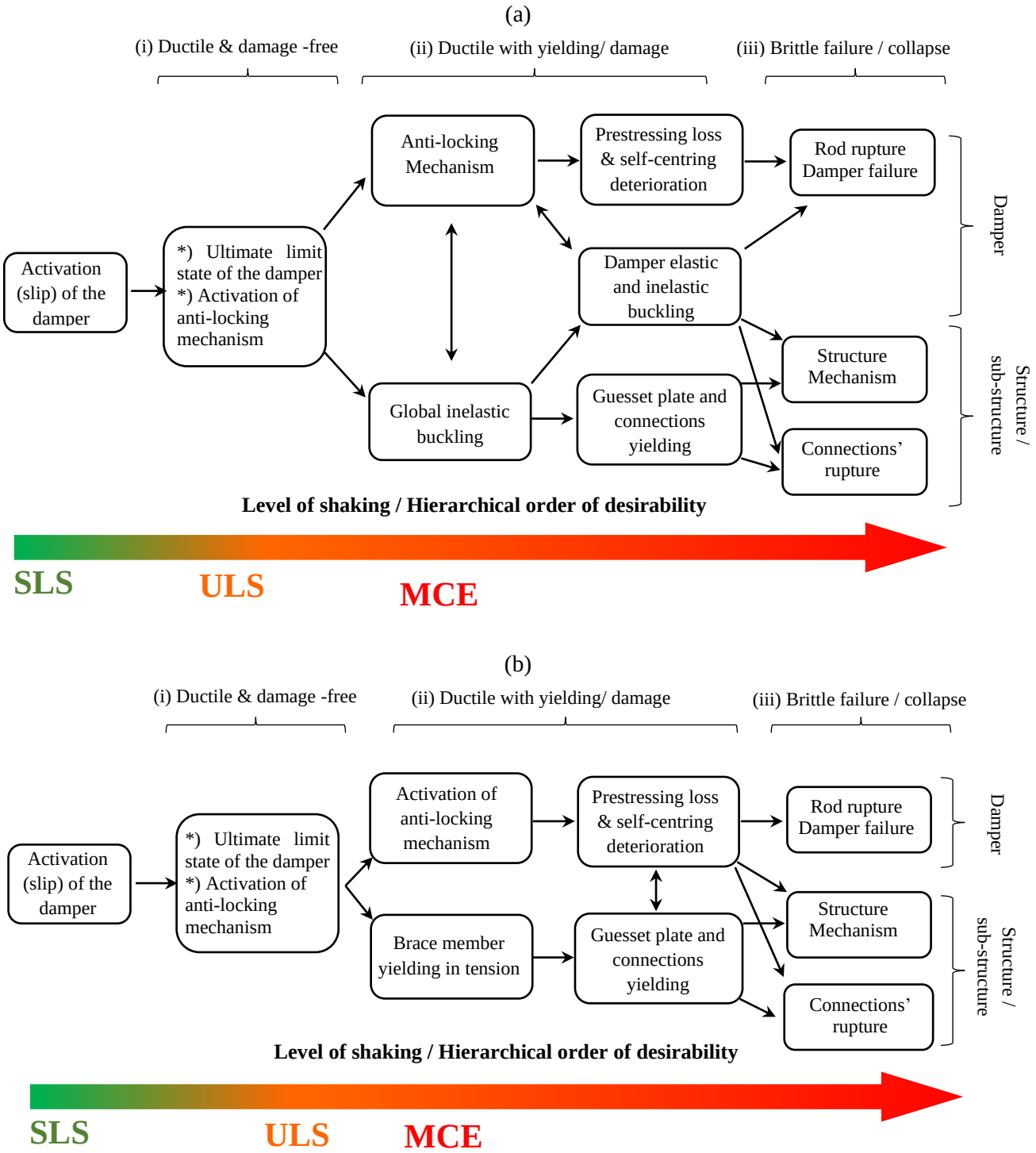

Figure 7: Failure modes associated with the RSFJ brace in a hierarchical order: (a) Compression and (b) Tension

5 CONCLUSION

The present paper reviewed and summarised the last four-year research program conducted at Auckland University of Technology and The University of Auckland on the RSFJ brace application. Based on the information to date, a number of failure modes associated with the RSFJ brace have been detected and analytically and experimentally investigated. It was observed that the failure modes can be categorized into two main groups in general namely: (a) local and (b) global instabilities. The local (localized) instability is associated with the damper being not able to transfer the axial compression fully while the global instability is

referred to the whole brace sub-assembly being not able to resist the axial compression perfectly. It was found that the local instability is greatly influenced by the boundary conditions of the damper (end support) while the global one is more sensitive to the damper and brace sectional and member properties. The global failure mode, itself, can be of two types, elastic and inelastic, depending on the length, geometry and characteristics of the brace and other components like anti-buckling tubes (ABTs). Another failure mode, nonlinear elastic buckling, was also observed but it was limited to the case where no ABT was used. A summary of the experimental observations and the associated analytical expressions were also provided. Finally, to give a big picture of the failure modes in a desirable order of occurrence, two flowcharts were proposed that can be used in combination with the capacity design procedure so that the desirable order of each failure mode is achieved.

6 ACKNOWLEDGEMENT

The authors would like to thank the Earthquake Commission (EQC) of New Zealand and the Ministry of Business, Innovation and Employment of New Zealand (MBIE) for the financial support provided for this research. Also, the contribution of technicians Allan Dixon, Andrew Virtue and Dave Croft, in the preparation of both test setups in Auckland University of Technology Built environment Lab are appreciated. The commercial interest for Tectonus Company providing the RSFJ specimens is acknowledged. The financial support from Aurecon company for the first author participation in the conference is appreciated.

7 REFERENCES

1. Yousef-Beik, S.M.M., P. Zarnani, F.M. Darani, A. Hashemi, and P. Quenneville. New seismic damage avoidant timber brace using innovative resilient slip friction joints for multi-story applications. in WCTE 2018 - World Conference on Timber Engineering. 2018.

2. Hashemi, A., B. Zaboli, S.M.M. Yousef-Beik, P. Zarnani, G.C. Clifton, and P. Quenneville, Seismic performance of resilient slip friction joint (RSFJ) brace with collapse prevention mechanism, in NZSEE 2018: Auckland.

3. Hashemi, A., S.M.M. Yousef-Beik, F.M. Darani, G.C. Clifton, P. Zarnani, and P. Quenneville, Seismic performance of a damage avoidance self-centring brace with collapse prevention mechanism. Journal of Constructional Steel Research, 2019. 155: p. 273-285.

4. Yousef-beik, S.M.M., S. Veismoradi, P. Zarnani, A. Hashemi, and P. Quenneville, Experimental Study on Cyclic Performance of a Damage-Free Brace with Self-Centering Connection. Journal of Structural Engineering, 2021. 147(1): p. 04020299.

5. Yousef-beik, S.M.M., P. Zarnani, A. Hashemi, and P. Quenneville, Lateral Instability of Self-centring Braces: Buckling in loading and Unloading, in Pacific Conference on Earthquake Engineering. 2019: Auckland, New Zealand.

6. Yousef-Beik, S.M.M., S. Varier, A. hashemi, P. Zarnani, and P. Quenneville, Design of RSFJ Self-centring Brace for Ultimate Limit State in NZSEE 2021. 2021: Christchurch, New Zealand.

7. Yousef-Beik, S.M.M., Development of a New Self-Centring Low-damage Bracing System for Earthquake Resistance Using Resilient Slip Friction Joints (RSFJ), in Department of Built Environment Engineering. 2021, Auckland University of Technology.

8. Yousef-beik, S.M.M., S. Veismoradi, P. Zarnani, and P. Quenneville, Effect of second-order actions on the performance of resilient slip friction joints: Analytical and experimental investigation. Structures, 2021. 33: p. 957-970.

9. Yousef-beik, S.M.M., H. Bagheri, P. Zarnani, A. Hashemi, and P. Quenneville, Damage-avoidance timber brace using a self-centring friction damper in Pacific Conference on Eathquake Engineering. 2019: Auckland, New Zealand.

10. Yousef-beik, S.M.M., H. Bagheri, S. Veismoradi, P. Zarnani, A. Hashemi, and P. Quenneville, Seismic performance improvement of conventional timber brace using re-centring friction connection. Structures, 2020. 26: p. 958-968.

11. Hashemi, A., S.M.M. Yousef-Beik, P. Zarnani, and P. Quenneville, Seismic strengthening of conventional timber structures using resilient braces. Structures, 2021. 32: p. 1619-1633.

12. Bažant, Z.P. and L. Cedolin, Stability of structures: elastic, inelastic, fracture and damage theories. 2010: World Scientific.

13. Chen, W.F. and E.M. Lui, Structural stability: theory and implementation. 1987.

14. Darani, F.M., P. Zarnani, S. Veismoradi, S.M.M. Yousef-beik, A. Hashemi, and P. Quenneville. Resilient slip friction joint performance: Component analysis, spring model and anti-locking mechanism. in Structures. 2021. Elsevier.

15. Bagheri, H., A. Hashemi, P. Zarnani, and P. Quenneville, The resilient slip friction joint tension-only brace beyond its ultimate level. Journal of Constructional Steel Research, 2020. 172: p. 106225.

16. Darani, F.M., P. Zarnani, S. Veismoradi, S.M.M. Yousef-beik, A. Hashemi, and P. Quenneville, Resilient slip friction joint performance: Component analysis, spring model and anti-locking mechanism. Structures, 2021. 33: p. 3897-3911.